Available online at www.ijournalse.org

Emerging Science Journal

(ISSN: 2610-9182)

Vol. 6, No. 4, August, 2022

Performance Improvement of Air-cooled Battery Thermal Management System using Sink of Different Pin-Fin Shapes

O. Miracle Oyewola [1*], A. Andrew Awonusi [2], O. Saheed Ismail [2]

[1] *School of Mechanical Engineering, Fiji National University, Suva, Fiji.*

[2] *Department of Mechanical Engineering, University of Ibadan, Ibadan, Nigeria.*

Abstract

One of the most important influences on battery safety, capacity, and cell ageing is heat generation and temperature inhomogeneity, which cause unbalanced ageing, resulting in cell performance decline. A well-developed temperature management module is required to avoid such undesirable actions. In this study, an air-cooled temperature management module was developed by coupling a unique heat sink of different pin-fin geometries/shapes to prismatic Li-ion cells and a 3D transient analysis was conducted to simulate the cooling performance of this heat sink under the effect of inlet airflow velocities and temperatures at a discharge rate of 2C for three cases. The results in the form of maximum temperature and temperature homogeneity inside the battery were derived and compared to the commonly used circular pin-fin heat sink. The overall result indicates that case 2, which consists of uniform height, shows better promise than others, taking into consideration the geometry employed. After 600 s and at a constant inlet air velocity of 0.412 m/s across a range of 20 ºC to 35 ºC, it was found that this heat sink performed better, providing an average of 1.87% and 1.93% improvement in temperature homogeneity and battery maximum temperature, respectively. Also, at a constant inlet air temperature of 27 ºC across the range of inlet air velocity of 0.206 m/s to 0.824 m/s, this heat sink provides an average of 1.77% and 0.27% improvement in temperature homogeneity and battery maximum temperature, respectively.

Keywords:

Battery Thermal Management System;
Lithium-ion Battery;
Heat Sink; Air Cooling.
Varied Pin-Fin Geometry;
Electric Vehicles;
Hybrid Electric Vehicles.

Article History:

Received:	10	December	2021
Revised:	28	April	2022
Accepted:	12	May	2022
Available online:	31	May	2022

1- Introduction

The adverse effects of climate change and pollution as a result of transportation activities on the environment and human health cannot be overemphasized. Technologies such as electric and hybrid electric vehicles have been introduced as a substitute for fossil fuel-driven vehicles to curb these effects. Rechargeable batteries are very essential for the smooth operation of some of these technologies. Lithium-ion (Li-ion) batteries have been noted to be a suitable candidate for these technologies. When compared to other types of rechargeable batteries in the same space, Li-ion batteries can store more electrical energy [1] and possess a longer life cycle [2].

It should be noted that, as with any operating rechargeable battery, heat is always generated, which causes the temperature to increase, and Li-ion batteries are very susceptible to operating temperature. This issue has been an area of concern and has attracted attention in recent times. For instance, several studies have recorded the effect of high temperatures on charge and discharge efficiency, output power, capacity degradation, and life of Li-ion batteries [3-6]. The interesting results that stemmed out of the past studies are to mitigate these temperature-rise effects and prevent thermal runaway. The Battery Thermal Management System (BTMS) is very essential to control the temperature rise and also maintain the lifelong durability of these batteries [7-9].

* **CONTACT**: olanrewaju.oyewola@fnu.ac.fj

DOI: http://dx.doi.org/10.28991/ESJ-2022-06-04-013

Different systems have been introduced for the Li-ion batteries for thermal management, among which are air and liquid cooling. However, air cooling has received much attention from researchers due to its simplicity in structure and implementation. In the research for air cooling, some of the primary areas of study are the air-flow pattern, cell arrangement, and inlet and outlet sections of the thermal battery management system. Peng et al. [10] numerically investigated the effects of several battery configurations, air inlet and outlet positions, and the number of inlets and outlets on a system. By revealing that a modest length-to-width ratio is more favorable to improving cooling system performance, we establish that the optimal arrangement for a 20-cylindrical cell battery pack is a 4 by 5 configuration. They also provided an 18 inlet and outlet placement layout where the layout allows fluid to flow over the majority of the battery pack over shorter distances, which is better for battery temperature management. It was also reported that the use of a large number of inlets and outlets allows for a more flexible fluid flow state. Similarly, Chen et al. [11] developed a symmetrical air-cooled system with an uneven cell-spacing distribution. The impact of battery cell quantity on the performance of an air-cooled system was first investigated numerically. The results revealed that a system with fewer battery cells can produce a more uniform temperature distribution and that each cell's energy consumption is lower. When asymmetrical and symmetrical parallel air-cooled Battery Thermal Management Systems (BTMSs) for prismatic batteries were compared in terms of thermal performance by analyzing various input and outlet positions, they discovered that symmetrical systems attain lower maximum temperatures and improve temperature uniformity. Fan et al. [12] analysed a module by employing a fan and a prismatic Li-ion battery. Using Computational Fluid Dynamics (CFD), it was discovered that increasing the fan flow rate as well as decreasing the gap resulted in a maximum temperature-rise decrease for the battery. Also, Liu et al. [13] used a shortcut computational method to talk about how the angle of the plenum plate, the distance between battery units, and the minimum width of the plenum affect the flow speed and temperature profile in a parallel air-cooled big battery pack.

The cooling capability of BTMS with various flow inlet and outlet locations has been extensively studied by many researchers. Chen et al. [14] studied the thermal performance of an air-cooled thermal management system with varying air inlet and outlet area placement; the results revealed that a battery thermal management system with air inlet and outlet placed at the middle of the plenum provides good cooling efficiency. Wang et al. [15] introduced parallel plates into the cooling channels of the system by altering the airflow distribution. They explored the influence of the number of parallel plates on the cooling performance of the BTMS; the result shows that the system with two parallel plates has the best cooling efficiency within the allowable range of power consumption loss, the effects of parallel plate length and height were further investigated; the best length and height values were 1.5 and 30 mm, respectively. Finally, these results were used to create three different optimization schemes for the model. Wang et al. [16] went further by introducing the parallel plates into 8 more airflow type BTMSs, which were simulated and evaluated for cooling performance. To begin with, a parallel plate was added to a standard Z-type BTMS, and the influence of the number of parallel plates on the battery pack's cooling performance was evaluated. The cooling efficiency of all BMTSs was then investigated and compared using four different schemes for adding parallel plates to each initial BTMS. The results showed that the strategy used in this study may significantly improve the BTMS' cooling efficiency. A unique J-type air-based BTMS was proposed by Liu et al. [17] that can be adaptively controlled by altering the two valves to achieve the best cooling performance.

Further studies have been conducted to improve the maximum temperature, maximum temperature difference, and/or power consumption. Li et al. [18] explored both numerical and experimental studies of a thermal management system consisting of a multi-cell battery pack and wind tunnel, from which a reduced-order model is created based on the verified CFD models to forecast the cell maximum temperature in the battery module. It was discovered that a reduced-order model's precision and simplicity made it attractive for in-situ monitoring and control. Employing a lumped-capacitance thermal model and a 2-D CFD model, Mahamud & Park [19] were able to numerically analyse a new thermal management approach using a reciprocating airflow for cylindrical Li-ion cell. Their result showed more cell maximum temperature and temperature difference reduction when operating on reciprocating flow as compared to uni-directional flow. It is worth noting that Giuliano et al. [20] developed a thermal management module using the air-cooling approach for a Lithium-titanate battery using metal foam-based heat exchanger plates. They found that the module can be an efficient and effective solution for cooling automobile battery packs. Meanwhile, Park [21] investigated the thermal performance of the present air-cooling battery system using the thermal resistance model; it was discovered that using the pressure relief ventilation and tapered manifold provides a suitable cooling performance.

On the other hand, liquid cooling has also been widely investigated by some researchers for some specific applications. For instance, several investigations have been conducted on the flow channel design and coolant thermal characteristics [22-25]. Recently, passive approaches such as phase change materials (PCM) and heat pipes have also received more interest. The consensus is that PCM successfully reduces average temperature and causes temperature homogeneity improvement for the Li-ion battery pack [26-28]. This is not surprising since heat pipes are known for their very high thermal conductivity, flexibility, long service life, and compact structure. In that respect, it has been shown to perform well for thermal management systems for Li-ion battery modules [2, 29-33].

Despite the progress made through the use of various cooling strategies for thermal management, few researches have been conducted on the effect of components such as spoilers [34, 35] and heat sink [1, 9] introduced into the air-cooled BTMS to improve the cooling performance of the system. There is a need to explore the design, modification, and optimization of these components inside the cooling systems to enhance better thermal management. Heat sinks of pin-fin with constant height and shape are useful components that have been utilized in a variety of cooling modules. They can greatly decrease the battery maximum temperature but are unlikely to enhance temperature homogeneity to an acceptable level [9]. In that respect, a unique cooling module is proposed in this study by employing a unique design of heat sink of pin-fin with different geometries (circular and square) (see Figure 1) to improve the thermal management of Li-ion battery pack by enhancing temperature homogeneity and maximum temperature reduction in the battery.

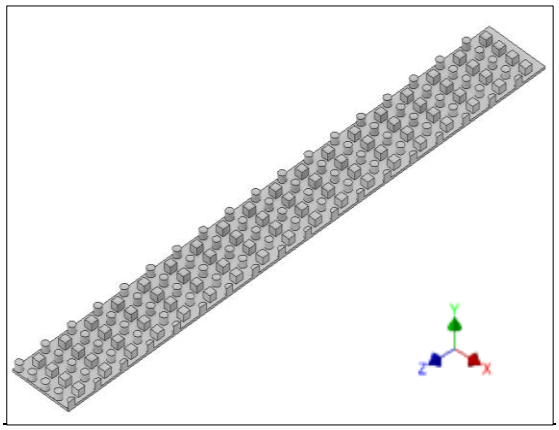

Figure 1. Section cut of the heat sink

Three (3) cases of the pin-fin heat sink design as regard variation in pin-fin height were introduced and studied. The effect of conditions such as inlet airflow velocities and temperatures on their thermal management responses inside the battery was investigated in a three-dimensional transient analysis of an air-cooled module containing the pin-fin heat sink coupled to prismatic Li-ion cells.

2- Problem Statement

Analysis was focused on a battery module of eight 15Ah prismatic cells [12]. To simplify the calculation and decrease computational cost and time, a symmetrical section of the battery (Figure 2) was evaluated. The optimum height of the airflow channel between the cells and Aluminum heat sink thickness was 3 mm [12] and 0.5 mm respectively. The pin-fin design on the heat sink is a combination of circular and square-shaped pins with the same hydraulic diameter of 2 mm. The pin-fin arrangement was staggered, with a longitudinal and transverse pitch to diameter ratios of 2 each.

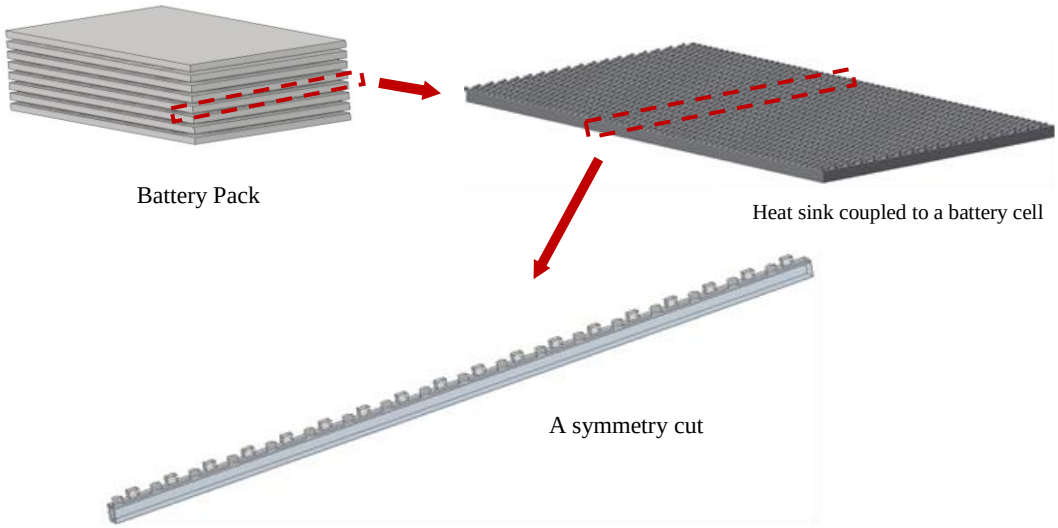

Figure 2. Thermal management system module

The symmetric section was cut along the width (145 mm) of the battery pack capturing the airflow channel, the symmetric cut of the heat sink, and the prismatic cell. The computational domain (Figure 3) is divided into 3 zones. (1) the airflow channel: housing the pin-fins, running from the inlet to the outlet boundary which was extended to contain

reverse flow during computation, (2) the heat sink: coupled to the air channel at the top and battery at its bottom, (3) the cell: the heat energy source. The main parameters of the cell are presented in Table 1.

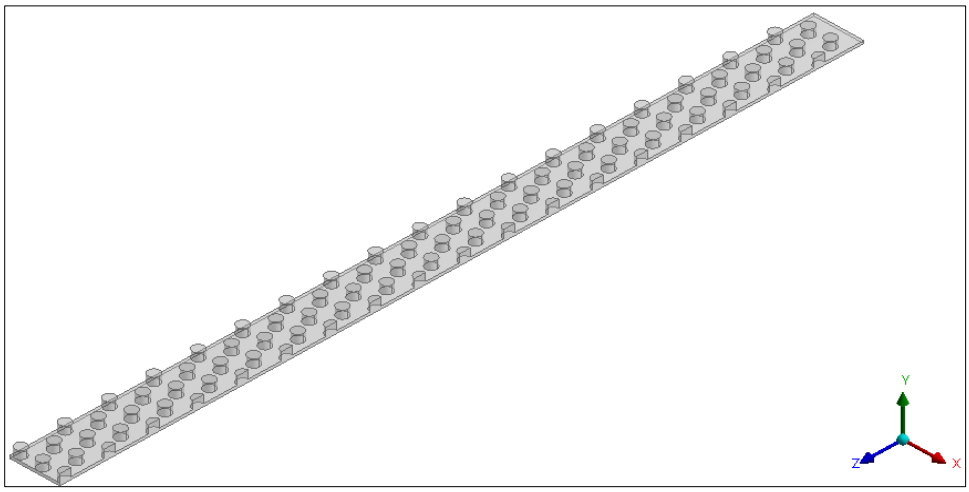

Case 1

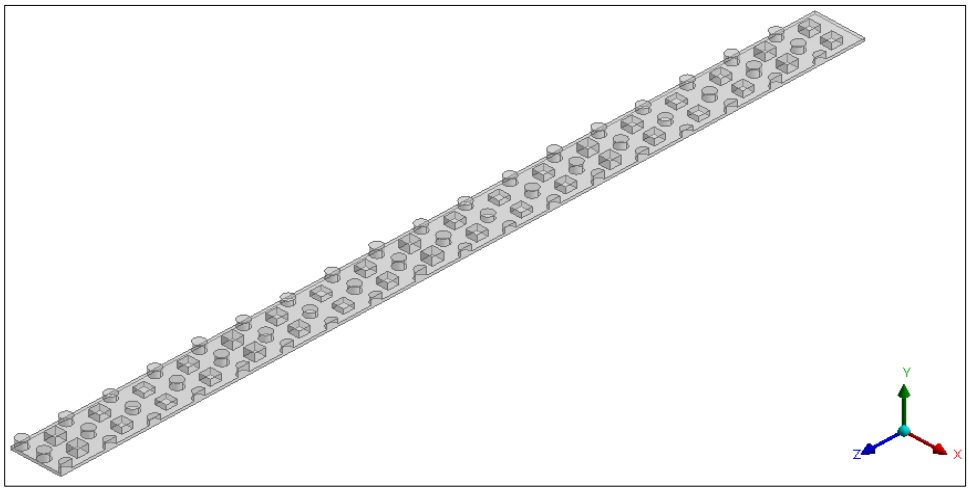

Case 2

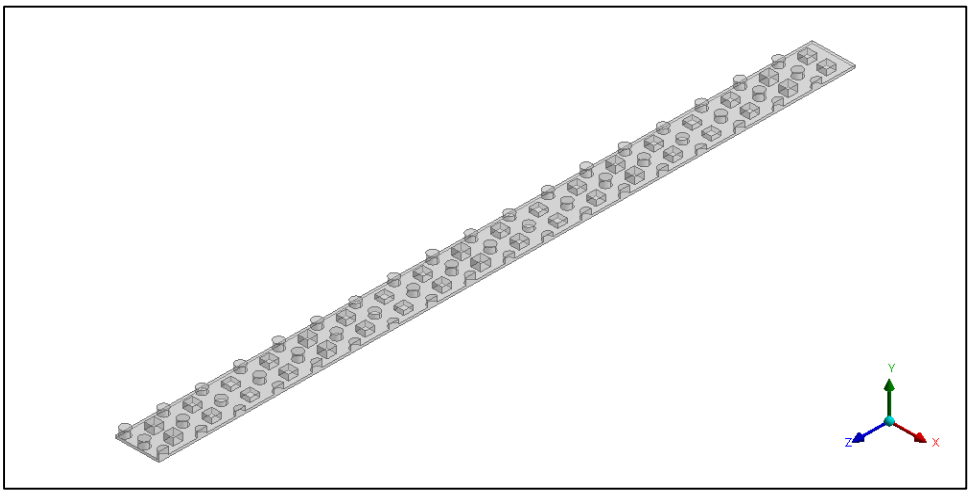

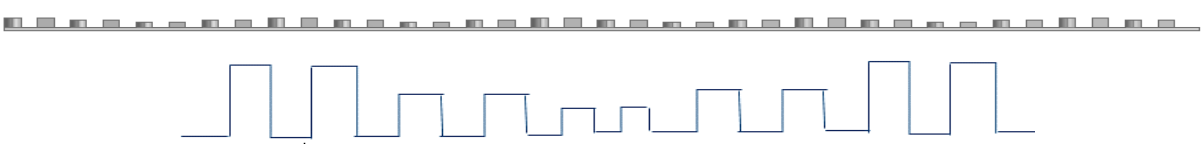

Case 3

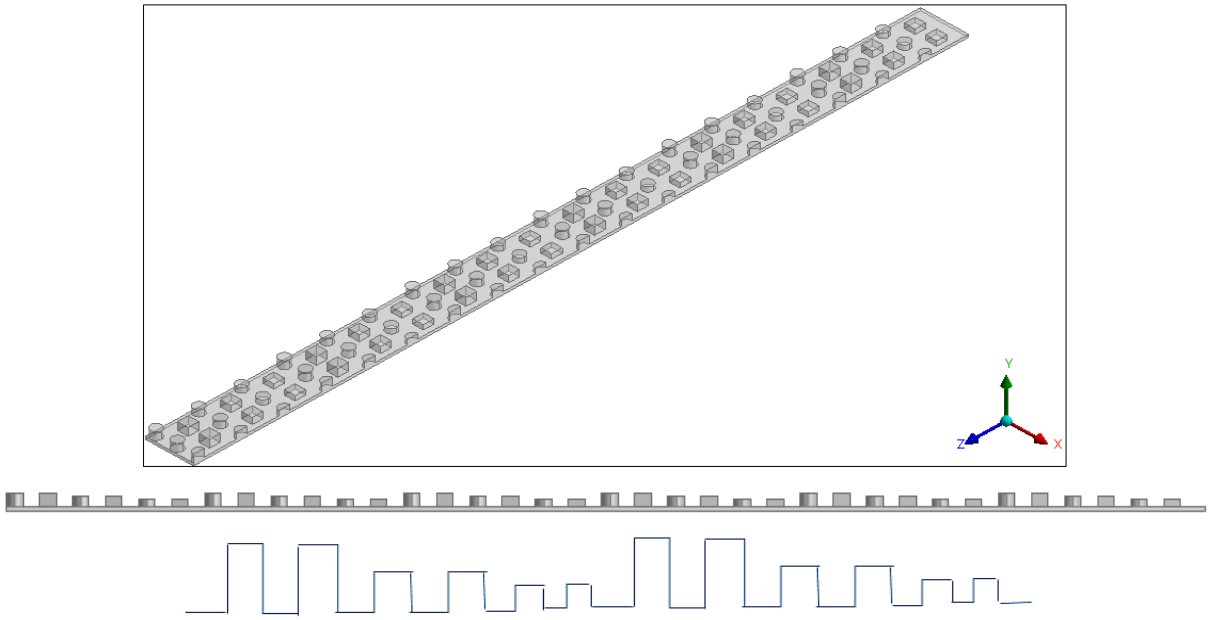

Case 4

Figure 3. Schematic and height variation pattern of cases 3 and 4

Table 1. The main properties of the battery cell [12]

Parameter	Value
Active area dimension (mm)	6 × 145 × 255
Heat specific capacity (J/Kg. K)	~745
Density (kg/m^3)	~2335
Thermal conductivity x, y, z (W/m. K)	~ (27, 0.8, 27)

Three (3) separate cases based on pin-fin height settings were investigated: the first setting (Case 2) has its pin-fins on a uniform height of 3 mm while the other two settings (Cases 3 and 4) have their arrangement set on a 3 stepwise height patterns of 3, 2.7, and 2.4 mm (see Figure 3). For comparison purposes, a circular pin-fin heat sink which is commonly used (Case 1) with a uniform height of 3mm was included against which all other cases can be assessed. The temperature homogeneity within the battery pack was quantified using the standard deviation of the temperature profile. Improved temperature homogeneity is depicted by lower standard deviation and the maximum temperature which will also be evaluated.

3- Mathematical Model

The thermodynamic energy balance on a Li-ion unit cell can be found in its simplified form as [36]:

$$q = I.(U - V) - I.\left(T\frac{\partial U}{\partial T}\right) \quad (1)$$

where q is the heat generation rate, I is the electric current, U is the open-circuit voltage, V is the cell voltage, T is the cell temperature, and ∂U/∂T is the temperature coefficient. The first term is the generated heat caused by electric current passing through internal resistances present in the cell while the second term is the generated or consumed heat in effect during discharge or charge cycle which is a product of cell electrochemical reaction [1, 37]. Using entropy change definition, Fathabadi [38] redeveloped Equation 1 to Equation 2:

$$\dot{q} = R_i.i^2 - i.T\frac{\Delta S}{F} \quad (2)$$

where $\dot{q}$ is the rate of internal heat generation per unit volume, i is the discharge current of a cell per unit volume, ΔS is the entropy change, and F is the Faraday number, 96485 C/mol. R_i is the internal equivalent resistance of the unit cell which is a function of temperature and SOC of the battery and are expressed as [38]:

$$R_i = \begin{cases} 2.258 \times 10^{-6} SOC^{-0.3952} & T = 20°C \\ 1.857 \times 10^{-6} SOC^{-0.2787} & T = 30°C \\ 1.659 \times 10^{-6} SOC^{-0.1692} & T = 40°C \end{cases} \quad (3)$$

From experimental results during the discharge cycle, it was discovered that ΔS is almost independent of temperature over a range of about 18ºC and 42ºC [38] and only a function of SOC:

$$\Delta S = \begin{cases} 99.88\,SOC - 76.67 & 0 \le SOC \le 0.77 \\ -30 & 0.77 \le SOC \le 0.87 \\ -20 & 0.87 \le SOC \le 1 \end{cases} \quad (4)$$

where SOC is defined as:

$$SOC = 1 - \frac{I.t}{C_0} \quad (5)$$

where C_0 is the electric capacity of the battery, t is the discharge duration, and I is the discharge current.

The flat Li-ion unit cell temperature distribution can be evaluated by employing the energy conservation equation [37, 38]:

$$\frac{1}{\alpha}\frac{\partial \mathrm{T}}{\partial \mathrm{t}} = \nabla^2 T + \frac{\dot{q}}{k} \quad (6)$$

where α and k are the thermal diffusivity and conductivity respectively. By substituting $\dot{q}$ from Equation 2 in Equation (6):

$$\nabla^2 T = \frac{1}{\alpha}\frac{\partial \mathrm{T}}{\partial \mathrm{t}} + \frac{\Delta S.i}{k.F}T - \frac{R_i.i^2}{k} \quad (7)$$

4- Numerical Method

Computational fluid dynamics techniques and algorithms have been widely used to design, analyse, and optimize equipment and/or processes involving fluid flow throughout the last three decades [9]. Boundary conditions were set up as shown in Figure 4 where the pressure outlet was set to atmospheric pressure. At the mesh interfaces between the airflow channel and the pin-fins and between the heat sink bottom and the battery top, a coupled wall was utilized to facilitate conjugate heat transfer. To ensure laminar flow, the analysis was conducted between inlet flow velocity of 0.206 m/s to 0.824 m/s. A discharge rate of 2C for all the simulations was utilized in this study. To investigate the effect of environmental conditions such as inlet velocity and temperature on the 3 cases at 600s, a parametric study was conducted and the cases were compared on their battery maximum temperature, temperature uniformity, and temperature difference inside the battery (maximum and minimum temperature). Figure 5 shows the step-by-step approach used for this study.

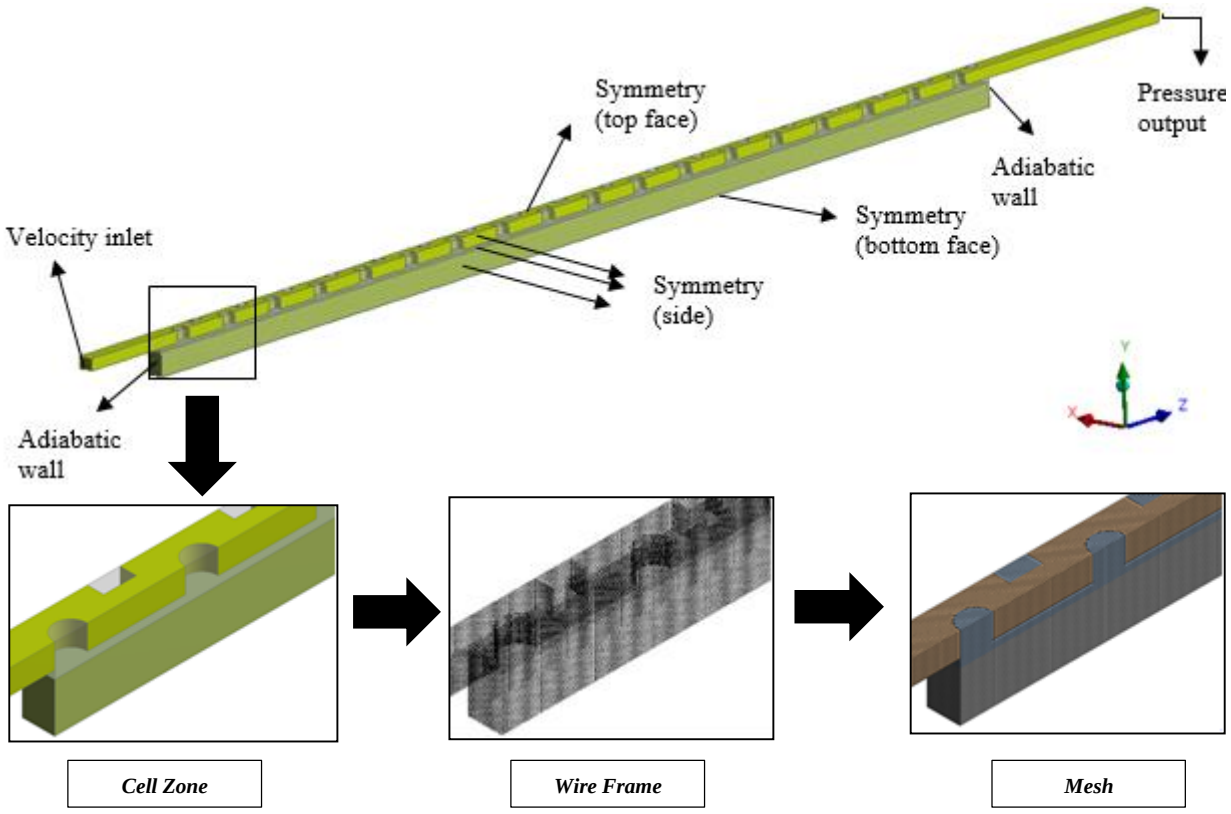

Figure 4. Computational domain setup

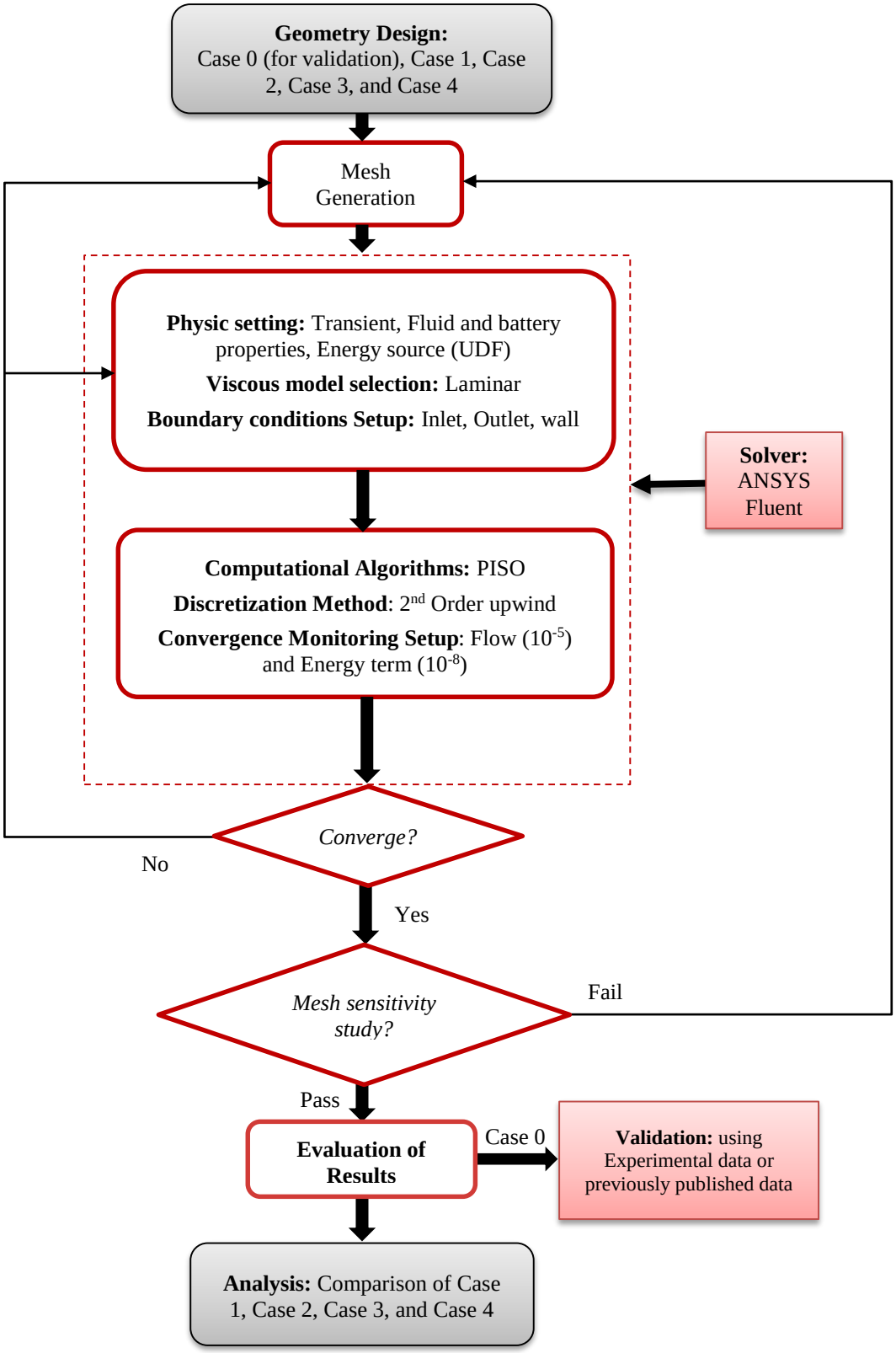

Figure 5. Methodology Flowchart

For simulation, a CFD software (*ANSYS Fluent*) was utilized under transient conditions, where the flow and thermal energy terms were discretized using second-order upwind and solved using PISO algorithms. This algorithm scheme has been noted to solve transient problems faster [1, 39]. After observing a grid sensitivity study, an adequate hexagonal cell sizing of 0.1462 mm was adopted over the whole computational domain. A 1s time step [1, 9] was set up for the integration of the governing equations. The residual convergence precisions for the velocity and heat energy were set at

10-5 and 10-8 respectively. To simulate the transient heat generation in the battery, a User Defined Function (UDF) was programmed following Equation 2 to Equation 5.

The numerical model allows for easy simulation of various flow and energy-generating processes and conditions, providing for more control over the physical process and the capacity to isolate certain phenomena for research. There are a few constraints (or assumptions), such as the fact that the physical properties of the air, as well as the ambient temperature and pressure, are constant during simulation conditions. Validation was observed by comparing the numerical solution of the model to that estimated by Mohammadin & Zhang [1] best design case which has been assigned as Case 0 in this study. The physical model (Case 0) used for the validation was a battery-coupled heat sink with circular pin-fin heights that rise linearly across the length of the heat sink. The simulated results were obtained at inlet flow velocity and temperature of 0.412 m/s, and 27 ºC, at t = 600s within the discharge rate of 1 - 5 ºC range. As a result, the model was chosen for the study as shown in Figure 6 which displays the comparison results where an average error of 7% was obtained which are in good agreement.

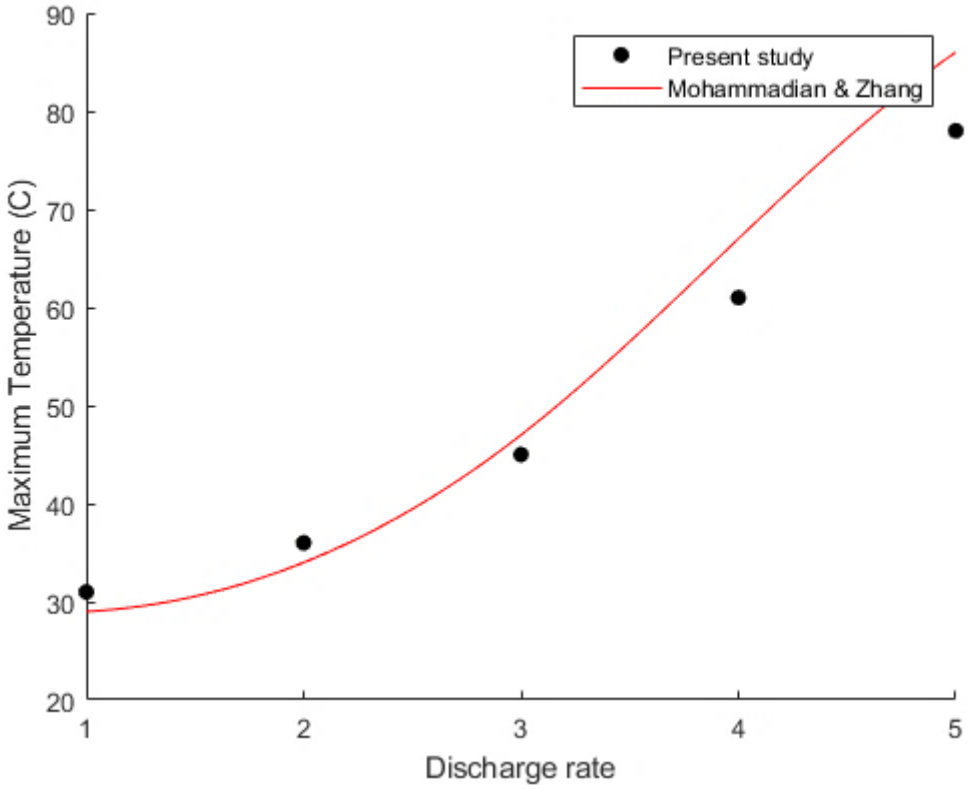

Figure 6. Model validation using battery maximum temperature at t = 600s

5- Results and Discussion

A unique type of heat sink of 2 different shapes of pin-fins coupled to a battery pack to constitute a thermal management system was studied and its performances under conditions such as inlet air velocities and temperature sink in decreasing the battery temperature standard deviation (i.e. temperature homogeneity) and the maximum temperature were observed.

The heat flux and temperature across the heat sink surface for different cases are shown in Figure 7. It can be observed that heat flux decreases across the interface and gradually dissipates as it approaches the end. As air travel across the heat sink, heat is being transferred to the air and its temperature increases thereby reducing the heat flux as it travels toward the end, little heat is being transferred to the air due to the small temperature difference between the air and heat sink. There is a steady temperature increase across the heat sink width which depicts the total temperature decrease inside the battery. Case 2 produces the highest cooling across the battery surface followed by Case 1. This suggests the presence of height uniformity of pin-fin across the heat sink in Case 1 and Case 2 providing enough surface area for heat transfer whereas Case 3 and Case 4 exhibit a poor cooling across the battery surface due to less surface area as a result of variation of their pin-fin height.

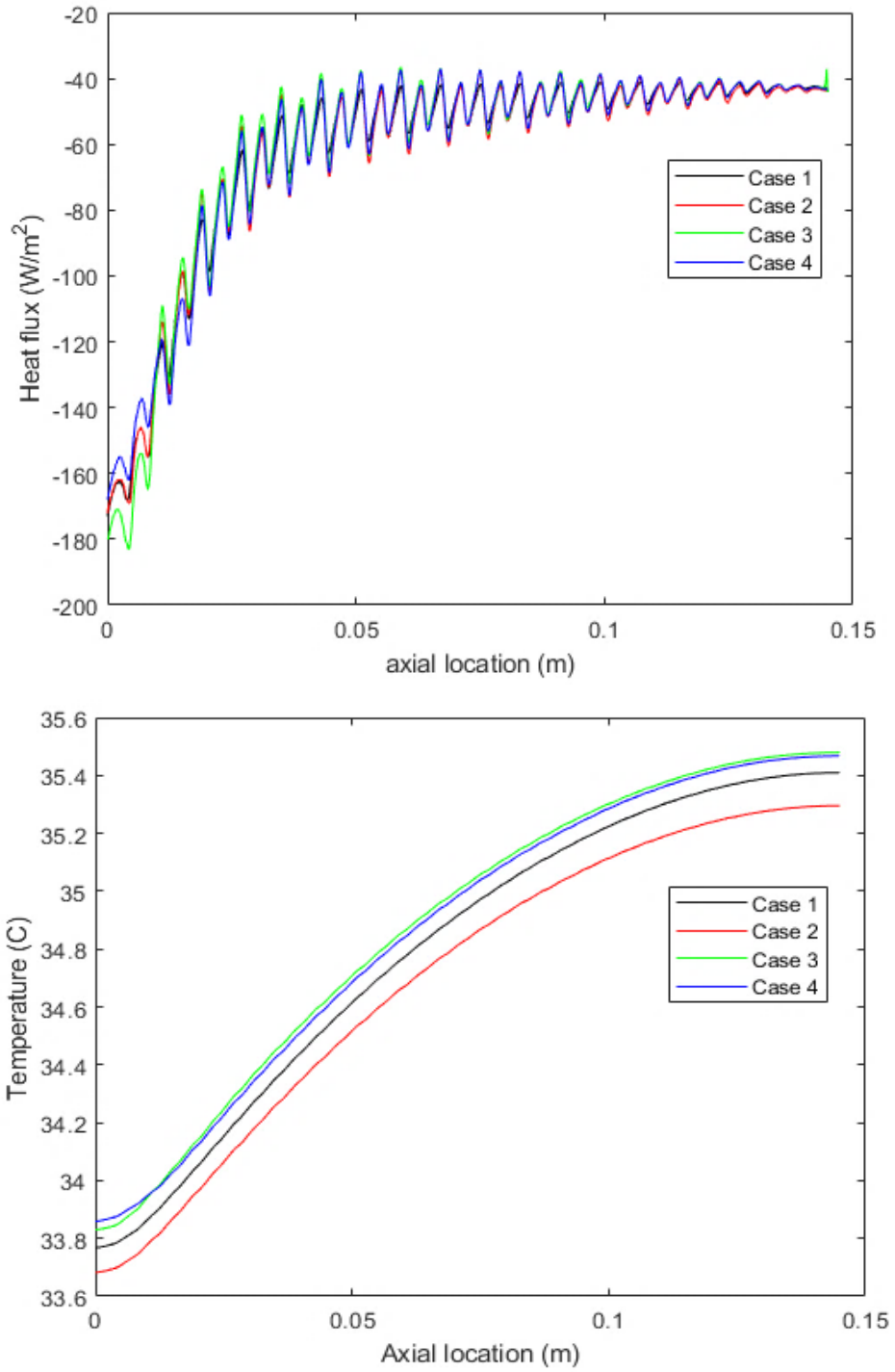

Figure 7. Variation of heat flux and surface temperature across the heat sink surface width for different cases at 0.412m/s, 27°C, and t = 600s

Figure 8 shows the maximum temperature and temperature uniformity at the inlet air temperatures. The battery maximum temperature increases as the temperature of the inlet air rises. There was impairment in the temperature uniformity inside the battery as the inlet air temperature increases which is depicted by an increase in the standard deviation of the temperature profile as the inlet air temperature increases. At a velocity of 0.412 m/s after 600s, it can be seen that Case 2 performs better under the variation as it causes the lowest maximum temperature to occur inside the battery and also offers the lowest standard deviation of the temperature field (improved temperature homogeneity). In comparison to Case 1, there is a percentage decrease of 2%, 2%, and 1.8% of battery maximum temperature and also a percentage decrease of 0.4%, 0.4%, and 4.8% of the standard deviation of the temperature profile at an inlet air temperature of 20ºC, 27ºC, and 35ºC respectively for Case 2. Interestingly, though the temperature homogeneity for Cases 3 and Case 4 was better when compared to that of Case 1, their batteries experience higher maximum temperatures which are not acceptable. The results may suggest that cases 3 and 4 also have good heat transfer characteristics but at the expense of the systems.

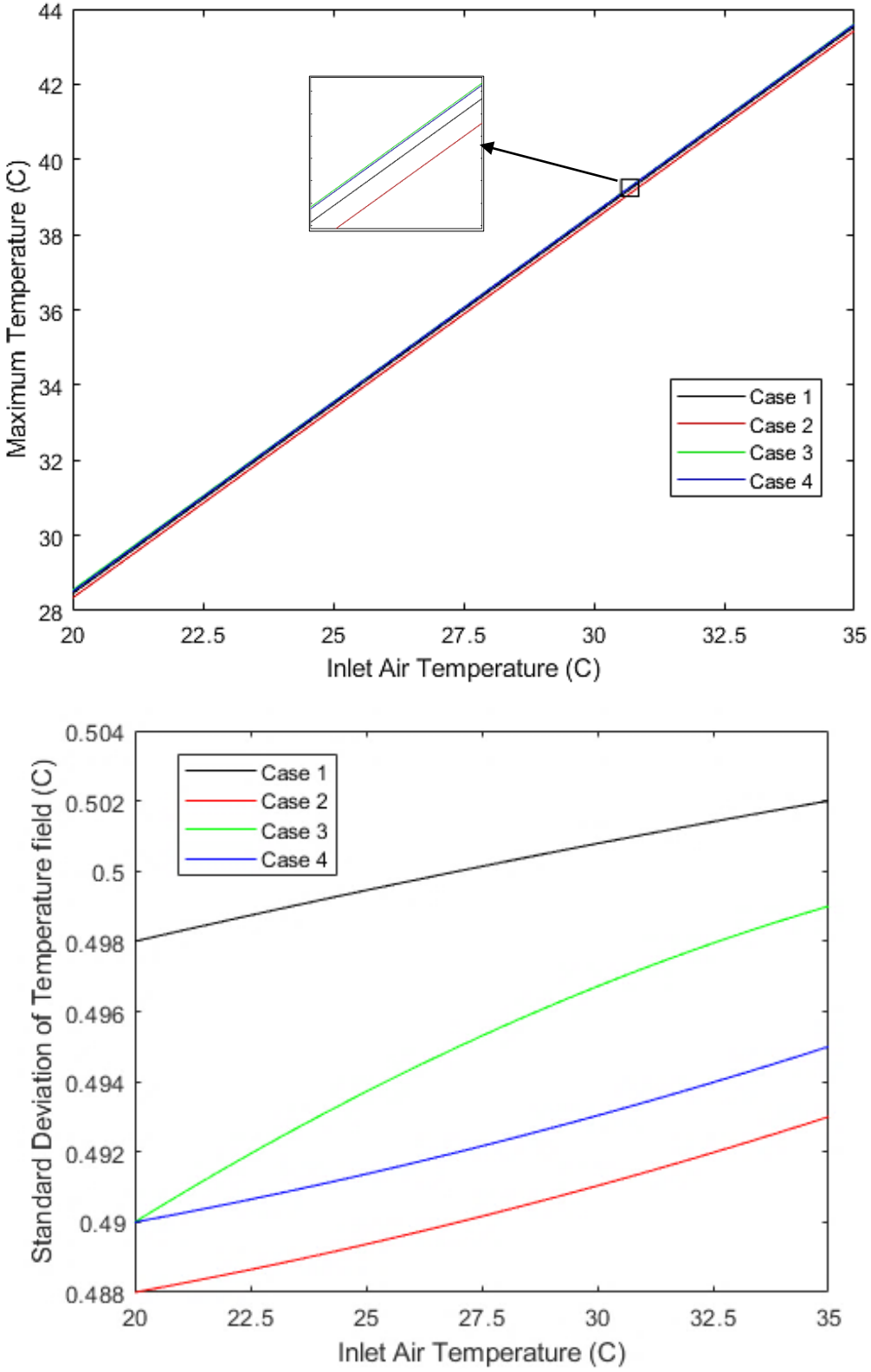

Figure 8. Battery maximum temperature and standard deviation of temperature profile against inlet air temperature for different cases at 0.412m/s and t = 600s

Figure 9 shows the battery maximum temperature and temperature homogeneity for different inlet air velocities. It shows that the maximum temperature decreases as the velocities of the inlet air increase. There was also impairment in the temperature homogeneity as the inlet air velocities increase which depicts that the standard deviation of the temperature profile increases as the inlet air velocity increases. At an inlet air temperature of 27°C after 600s, it is observed that Case 2 provides the best choice as its battery possessed the lowest maximum temperature and a better improvement in its temperature homogeneity. This is not surprising; the effect suggests the role of height uniformity in the heat transfer characteristics in enhancing cooling structures.

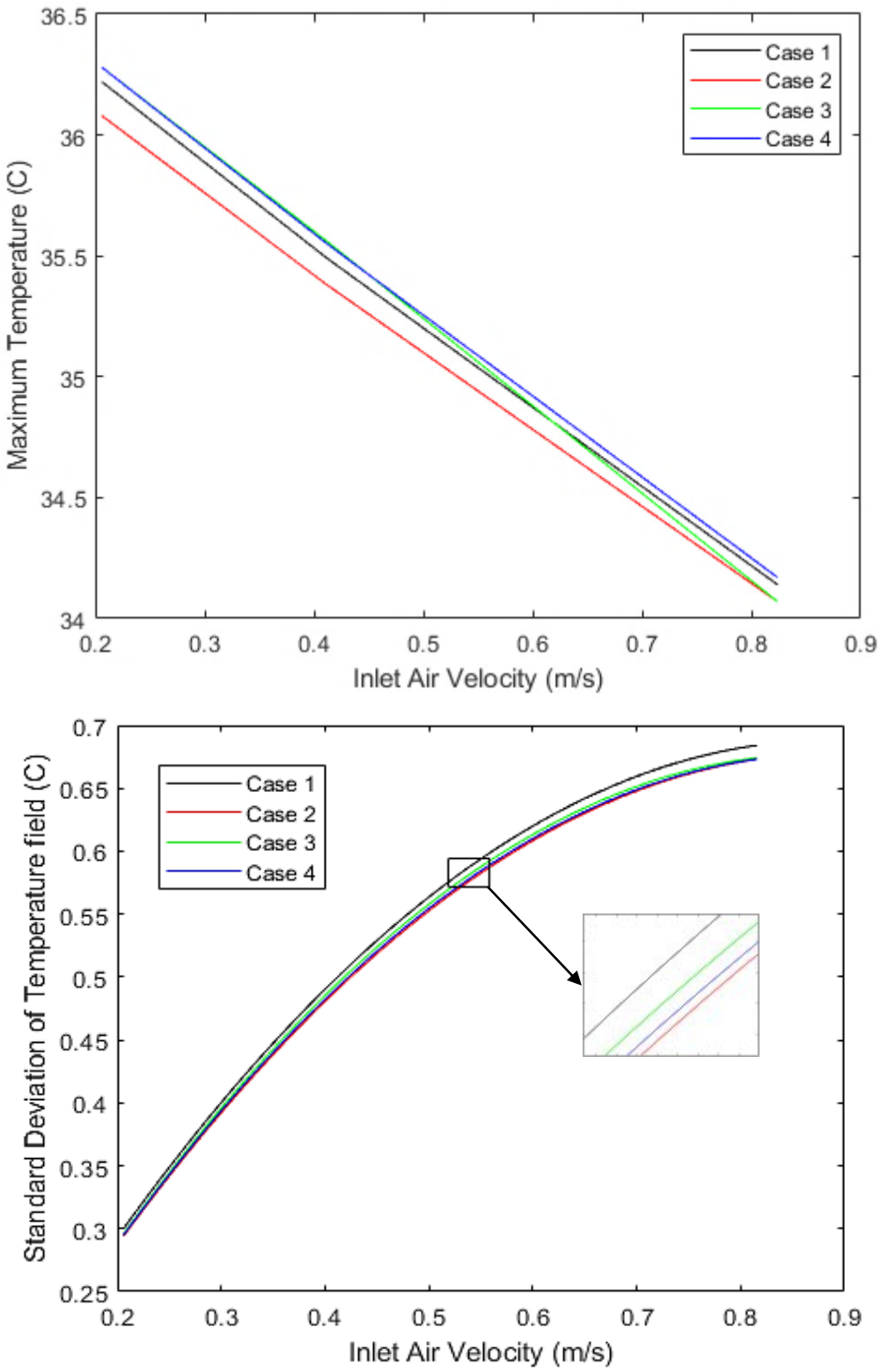

Figure 9. Battery maximum temperature and standard deviation of temperature profile against inlet air velocity for different cases at 27°C and t = 600s

Interestingly, as the velocity increases, the maximum temperature of Case 3 and Case 4 drop drastically, with Case 3 surpassing that of Case 1 at 0.62 m/s and meeting Case 2 at 0.824 m/s. This could be due to the airflow at higher velocity losing less energy when encountering fewer obstacles as a result of the variation in the pin-fin height thereby causing more heat transfer. Results showed that the standard deviation of the temperature profile increases as the inlet air velocities increase, which suggests that the temperature homogeneity is impaired (see Figure 9). However, the studies of Mohammadin & Zhang [1], and Fan et al. [10] showed that as the inlet air velocity increases, the standard deviation of the temperature profile reaches a peak and declines leading to improvement in the temperature uniformity. This is not surprising; all the cases in this present study follow similar behaviour under the conditions of increasing the inlet air

velocity. It should be noted that, with reference to Case 1, there is a percentage decrease of 0.3%, 0.3%, and 0.2% of maximum temperature in the battery and also a percentage decrease of 2%, 2%, and 1.3% of the standard deviation of the temperature profile at inlet air velocities of 0.206 m/s, 0.412 m/s, and 0.824 m/s respectively for Case 2.

The main aim of Mohammadin & Zhang [1] in introducing a variation of pin-fin height in their study is to reduce the standard deviation of temperature in a battery which inspired the introduction of variation in the pin-fin height for two of the cases (Case 3 and Case 4) in this study. Within the studied conditions of inlet air temperature and velocity, Case 2 provided the best cooling design of the four cases both in offering the lowest maximum temperature and standard deviation of temperature in the battery. At similar conditions of 2C discharge rate at an inlet air temperature of 27ºC and different inlet air velocities for 600s, Figure 10 shows the comparison of Case 2 and Mohammadin & Zhang's [1] best case which is a heat sink design of circular pin-fin height that rise linearly across the length of the heat sink. For the standard deviation of the temperature, Case 2 performs better with an average percentage decrease of 23%. As regard the maximum temperature, Case 2 lag behind by an average of 1.8%.

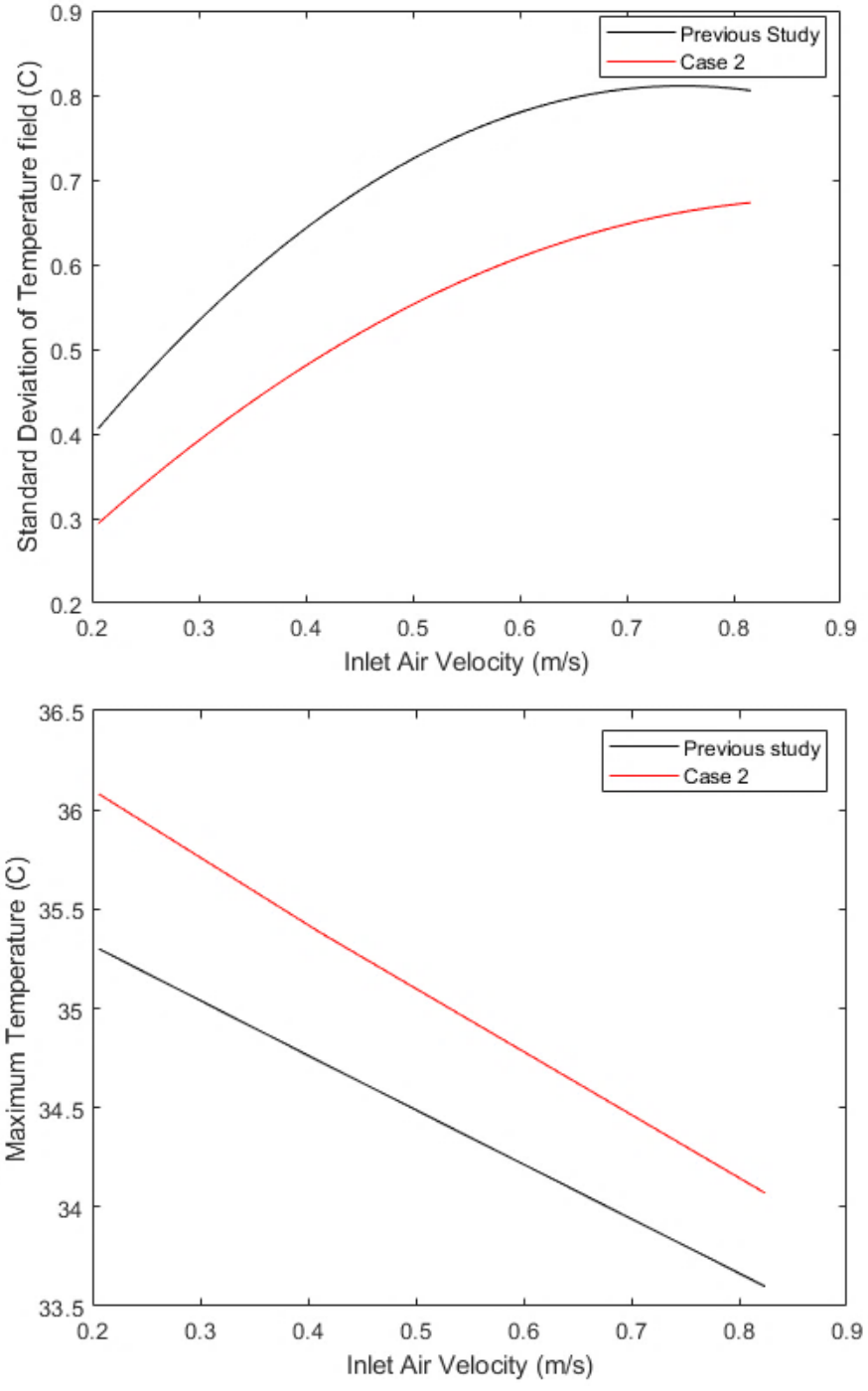

Figure 10. Comparison of Case 2 with a previous study under different inlet air velocities at 27ºC, 2C discharge rate and t = 600s

Figure 11 displays the temperature profile in the battery for different cases after 600 s at an inlet air velocity and temperature of 0.412 m/s and 27ºC respectively. The temperature is minimum at the battery surface close to the channel inlet and maximum down the battery toward the channel outlet. This might be due to the temperature difference between the airflow temperature at the channel inlet and the coupled heat sink. This is not surprising since the coupled heat sink is at a higher temperature, causing more heat transfer to take place in that region. However, as the airflow toward the outlet increased, the temperature difference dropped due to the increase in the airflow temperature, which results in less heat transfer out of the battery as the air flows out. The effect of this is reflected in all the cases. However, the difference between the battery minimum and maximum temperature point is the lowest for Case 2, suggesting a better performance taking into consideration the geometry.

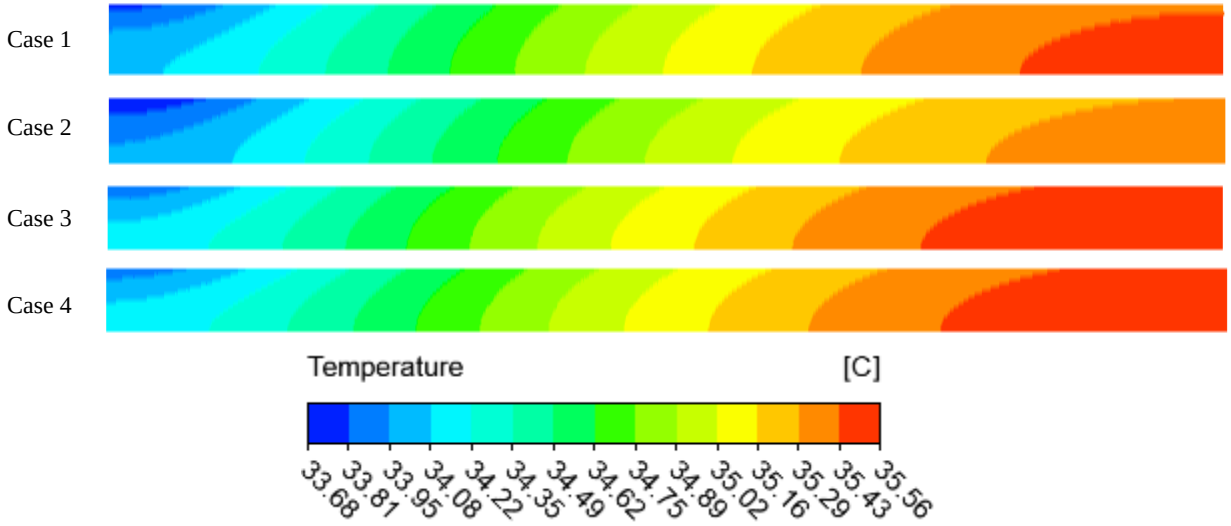

Figure 11. Temperature distribution in the battery for different cases for inlet airflow of 0.412m/s at 27ºC after 600s

6- Conclusion

A three-dimensional CFD transient analysis was conducted on an air-cooled thermal management module of a Li-ion battery coupled to a unique type of heat sink with two different pin-fin geometries (circular and square). Case studies as regards the pin-fin height variation were developed to study the cooling performance of the heat sink on the battery under the effect of inlet flow velocities and temperatures at a discharge rate of 2C after 600 s into the thermal management module. The variation in pin-fin shape (circular and square) of a heat sink shows better cooling performance than that of a commercial circular pin-fin. It was found that, although Cases 3 and 4 performed better as regard to temperature homogeneity inside the battery, their battery maximum temperatures were higher, which was unacceptable. Overall results favoured Case 2 (heat sink of different pin-fin shapes of constant height) as the best choice compared to others, and in addition, it performed better than the circular pin fin heat sink. It offers a 2% improvement in thermal homogeneity under constant velocity of 0.412 m/s within the studied inlet air temperatures and a 1.8% improvement under constant temperature of 27ºC within the studied inlet air velocities. This heat sink provides a 23% improvement in thermal homogeneity than a heat sink of varying pin-fin height designed for thermal homogeneity purposes conducted by a previous study. Case 2 offers more improvement in thermal homogeneity, which is essential in the battery thermal management system of electric and hybrid electric vehicles. The scope of this study was limited to the laminar flow of air into the thermal management module, future work may be considered on the effect of turbulent flow on the cooling performance of the heat sink as the study shows that Case 3 and Case 4 improve drastically as higher air velocity gets involved. Also, work may be considered on the cooling performance of a heat sink with variations of other different pin-fin shape combinations.

7- Declarations

7-1- Author Contributions

Conceptualization, O.O.; methodology, O.O., A.A. and O.I.; software, O.O. and A.A.; validation, O.O., A.A. and O.I.; formal analysis, O.O. and A.A.; investigation, O.O., A.A. and O.I.; resources, O.O.; data curation, O.O., A.A. and O.I.; writing—original draft preparation, O.O., A.A. and O.1.; writing—review and editing, O.O. and O.I.; visualization, O.O. and A.A.; supervision, O.O. and O.I.; project administration, O.O. All authors have read and agreed to the published version of the manuscript.

7-2- Data Availability Statement

The data presented in this study are available on request from the corresponding author.

7-3- Funding

The authors received no financial support for the research, authorship, and/or publication of this article.

7-4- Conflicts of Interest

The authors declare that there is no conflict of interest regarding the publication of this manuscript. In addition, the ethical issues, including plagiarism, informed consent, misconduct, data fabrication and/or falsification, double publication and/or submission, and redundancies have been completely observed by the authors.

8- References

[1] Mohammadian, S. K., & Zhang, Y. (2015). Thermal management optimization of an air-cooled Li-ion battery module using pin-fin heat sinks for hybrid electric vehicles. Journal of Power Sources, 273, 431–439. doi:10.1016/j.jpowsour.2014.09.110.

[2] Behi, H., Behi, M., Karimi, D., Jaguemont, J., Ghanbarpour, M., Behnia, M., Berecibar, M., & Van Mierlo, J. (2021). Heat pipe air-cooled thermal management system for lithium-ion batteries: High power applications. Applied Thermal Engineering, 183. doi:10.1016/j.applthermaleng.2020.116240.

[3] Sun, J., Li, J., Zhou, T., Yang, K., Wei, S., Tang, N., Dang, N., Li, H., Qiu, X., & Chen, L. (2016). Toxicity, a serious concern of thermal runaway from commercial Li-ion battery. Nano Energy, 27, 313–319. doi:10.1016/j.nanoen.2016.06.031.

[4] Wang, Q., Jiang, B., Li, B., & Yan, Y. (2016). A critical review of thermal management models and solutions of lithium-ion batteries for the development of pure electric vehicles. Renewable and Sustainable Energy Reviews, 64, 106–128. doi:10.1016/j.rser.2016.05.033.

[5] Miranda, Á. G., & Hong, C. W. (2013). Integrated modeling for the cyclic behavior of high power Li-ion batteries under extended operating conditions. Applied Energy, 111, 681–689. doi:10.1016/j.apenergy.2013.05.047.

[6] Ye, Y., Shi, Y., & Tay, A. A. O. (2012). Electro-thermal cycle life model for lithium iron phosphate battery. Journal of Power Sources, 217, 509–518. doi:10.1016/j.jpowsour.2012.06.055.

[7] Kizilel, R., Sabbah, R., Selman, J. R., & Al-Hallaj, S. (2009). An alternative cooling system to enhance the safety of Li-ion battery packs. Journal of Power Sources, 194(2), 1105–1112. doi:10.1016/j.jpowsour.2009.06.074.

[8] Saw, L. H., Ye, Y., Yew, M. C., Chong, W. T., Yew, M. K., & Ng, T. C. (2017). Computational fluid dynamics simulation on open cell aluminium foams for Li-ion battery cooling system. Applied Energy, 204, 1489–1499. doi:10.1016/j.apenergy.2017.04.022.

[9] Mohammadian, S. K., & Zhang, Y. (2017). Cumulative effects of using pin fin heat sink and porous metal foam on thermal management of lithium-ion batteries. Applied Thermal Engineering, 118, 375–384. doi:10.1016/j.applthermaleng.2017.02.121.

[10] Peng, X., Cui, X., Liao, X., & Garg, A. (2020). A thermal investigation and optimization of an air-cooled lithium-ion battery pack. Energies, 13(11), 2956. doi:10.3390/en13112956.

[11] Chen, K., Chen, Y., She, Y., Song, M., Wang, S., & Chen, L. (2020). Construction of effective symmetrical air-cooled system for battery thermal management. Applied Thermal Engineering, 166, 114679. doi:10.1016/j.applthermaleng.2019.114679.

[12] Fan, L., Khodadadi, J. M., & Pesaran, A. A. (2013). A parametric study on thermal management of an air-cooled lithium-ion battery module for plug-in hybrid electric vehicles. Journal of Power Sources, 238, 301–312. doi:10.1016/j.jpowsour.2013.03.050.

[13] Liu, Z., Wang, Y., Zhang, J., & Liu, Z. (2014). Shortcut computation for the thermal management of a large air-cooled battery pack. Applied Thermal Engineering, 66(1–2), 445–452. doi:10.1016/j.applthermaleng.2014.02.040.

[14] Chen, K., Wu, W., Yuan, F., Chen, L., & Wang, S. (2019). Cooling efficiency improvement of air-cooled battery thermal management system through designing the flow pattern. Energy, 167, 781–790. doi:10.1016/j.energy.2018.11.011.

[15] Wang, M., Hung, T. C., & Xi, H. (2021). Numerical study on performance enhancement of the air-cooled battery thermal management system by adding parallel plates. Energies, 14(11), 3096. doi:10.3390/en14113096.

[16] Wang, M., Teng, S., Xi, H., & Li, Y. (2021). Cooling performance optimization of air-cooled battery thermal management system. Applied Thermal Engineering, 195, 117242. doi:10.1016/j.applthermaleng.2021.117242.

[17] Liu, Y., & Zhang, J. (2019). Design a J-type air-based battery thermal management system through surrogate-based optimization. Applied Energy, 252, 113426. doi:10.1016/j.apenergy.2019.113426.

[18] Li, X., He, F., & Ma, L. (2013). Thermal management of cylindrical batteries investigated using wind tunnel testing and computational fluid dynamics simulation. Journal of Power Sources, 238, 395–402. doi:10.1016/j.jpowsour.2013.04.073.

[19] Mahamud, R., & Park, C. (2011). Reciprocating air flow for Li-ion battery thermal management to improve temperature uniformity. Journal of Power Sources, 196(13), 5685–5696. doi:10.1016/j.jpowsour.2011.02.076.

[20] Giuliano, M. R., Prasad, A. K., & Advani, S. G. (2012). Experimental study of an air-cooled thermal management system for high capacity lithium-titanate batteries. Journal of Power Sources, 216, 345–352. doi:10.1016/j.jpowsour.2012.05.074.

[21] Park, H. (2013). A design of air flow configuration for cooling lithium ion battery in hybrid electric vehicles. Journal of Power Sources, 239, 30–36. doi:10.1016/j.jpowsour.2013.03.102.

[22] Qian, Z., Li, Y., & Rao, Z. (2016). Thermal performance of lithium-ion battery thermal management system by using mini-channel cooling. Energy Conversion and Management, 126, 622–631. doi:10.1016/j.enconman.2016.08.063.

[23] Basu, S., Hariharan, K. S., Kolake, S. M., Song, T., Sohn, D. K., & Yeo, T. (2016). Coupled electrochemical thermal modelling of a novel Li-ion battery pack thermal management system. Applied Energy, 181, 1–13. doi:10.1016/j.apenergy.2016.08.049.

[24] Wu, F., & Rao, Z. (2017). The lattice Boltzmann investigation of natural convection for nanofluid based battery thermal management. Applied Thermal Engineering, 115, 659–669. doi:10.1016/j.applthermaleng.2016.12.139.

[25] Patil, M. S., Seo, J. H., Panchal, S., Jee, S. W., & Lee, M. Y. (2020). Investigation on thermal performance of water-cooled Li-ion pouch cell and pack at high discharge rate with U-turn type microchannel cold plate. International Journal of Heat and Mass Transfer, 155, 119728. doi:10.1016/j.ijheatmasstransfer.2020.119728.

[26] Ling, Z., Chen, J., Fang, X., Zhang, Z., Xu, T., Gao, X., & Wang, S. (2014). Experimental and numerical investigation of the application of phase change materials in a simulative power batteries thermal management system. Applied Energy, 121, 104–113. doi:10.1016/j.apenergy.2014.01.075.

[27] Javani, N., Dincer, I., Naterer, G. F., & Rohrauer, G. L. (2014). Modeling of passive thermal management for electric vehicle battery packs with PCM between cells. Applied Thermal Engineering, 73(1), 307–316. doi:10.1016/j.applthermaleng.2014.07.037.

[28] Javani, N., Dincer, I., Naterer, G. F., & Yilbas, B. S. (2014). Heat transfer and thermal management with PCMs in a Li-ion battery cell for electric vehicles. International Journal of Heat and Mass Transfer, 72, 690–703. doi:10.1016/j.ijheatmasstransfer.2013.12.076.

[29] Behi, H., Karimi, D., Behi, M., Ghanbarpour, M., Jaguemont, J., Sokkeh, M. A., Gandoman, F. H., Berecibar, M., & Van Mierlo, J. (2020). A new concept of thermal management system in Li-ion battery using air cooling and heat pipe for electric vehicles. Applied Thermal Engineering, 174, 115280. doi:10.1016/j.applthermaleng.2020.115280.

[30] Dan, D., Yao, C., Zhang, Y., Zhang, H., Zeng, Z., & Xu, X. (2019). Dynamic thermal behavior of micro heat pipe array-air cooling battery thermal management system based on thermal network model. Applied Thermal Engineering, 162, 114183. doi:10.1016/j.applthermaleng.2019.114183.

[31] Ye, X., Zhao, Y., & Quan, Z. (2018). Experimental study on heat dissipation for lithium-ion battery based on micro heat pipe array (MHPA). Applied Thermal Engineering, 130, 74–82. doi:10.1016/j.applthermaleng.2017.10.141.

[32] Ye, Y., Saw, L. H., Shi, Y., & Tay, A. A. O. (2015). Numerical analyses on optimizing a heat pipe thermal management system for lithium-ion batteries during fast charging. Applied Thermal Engineering, 86, 281–291. doi:10.1016/j.applthermaleng.2015.04.066.

[33] Tran, T. H., Harmand, S., Desmet, B., & Filangi, S. (2014). Experimental investigation on the feasibility of heat pipe cooling for HEV/EV lithium-ion battery. Applied Thermal Engineering, 63(2), 551–558. doi:10.1016/j.applthermaleng.2013.11.048.

[34] Zhang, F., Lin, A., Wang, P., & Liu, P. (2021). Optimization design of a parallel air-cooled battery thermal management system with spoilers. Applied Thermal Engineering, 182, 116062. doi:10.1016/j.applthermaleng.2020.116062.

[35] Wang, N., Li, C., Li, W., Huang, M., & Qi, D. (2021). Effect analysis on performance enhancement of a novel air cooling battery thermal management system with spoilers. Applied Thermal Engineering, 192, 116932. doi:10.1016/j.applthermaleng.2021.116932.

[36] Gu, W. B., & Wang, C. Y. (2000). Thermal-Electrochemical Modeling of Battery Systems. Journal of the Electrochemical Society, 147(8), 2910. doi:10.1149/1.1393625.

[37] Karimi, G., & Li, X. (2013). Thermal management of lithium-ion batteries for electric vehicles. International Journal of Energy Research, 37(1), 13–24. doi:10.1002/er.1956.

[38] Fathabadi, H. (2014). A novel design including cooling media for Lithium-ion batteries pack used in hybrid and electric vehicles. Journal of Power Sources, 245, 495–500. doi:10.1016/j.jpowsour.2013.06.160.

[39] ANSYS. (2010). Introduction to ANSYS Fluent. ANSYS Customer Training Material, 1–59. Available online: https://imechanica.org/files/fluent_13.0_lecture10-transient.pdf (accessed on January 2022).